

Integrated Localization and Control for Accurate Multi-Agent Formation

Yang Cai and Yuan Shen

Tsinghua National Laboratory for Information Science and Technology
Department of Electronic Engineering, Tsinghua University, Beijing 100084, China
Email: caiyang15@mails.tsinghua.edu.cn, shenyuan_ee@tsinghua.edu.cn

Abstract—High-accuracy formation is of great significance for multi-agent systems to perform complex tasks, and the accuracy of the formation is determined jointly by the network localization and formation control procedures. Existing studies commonly treat the two procedures separately and do not exploit an integrated design, leading to suboptimal formation performance. This paper establishes a general framework for high-accuracy multi-agent formation by integrated localization and control. In particular, we first propose a new metric called formation error to characterize the minimum squared distance between a real formation and a target one over arbitrary translation and rotation. Then we develop an integrated localization and control scheme to minimize the formation error. In the case study, we design the minimum mean formation error control algorithm along with a specific link selection strategy. Numerical results validate the performance gain of the integrated scheme over existing methods, and demonstrate effects of system parameters, which can serve as a guideline for practical system design.

I. INTRODUCTION

Multi-agent systems can accomplish numerous complicated missions, such as target tracking, cooperative combat and stereo reconstruction, of which a single agent is hardly capable [1], [2]. Specially, there is a growing tendency of using swarms of unmanned aerial vehicles (UAV) to perform confidential or dangerous tasks in predefined formations, which raised an urgent demand for approaches of high-accuracy multi-agent formation. The realization of the goal relies crucially on the position information, which can be acquired with the aid of localization techniques. The global positioning system (GPS), however, only provides location estimation of limited precision, and does not operate well in harsh environments with high interference or obstacle shadowing. Cooperative localization among agents addresses the drawbacks, and thus can aid the application of multi-agent formation [3].

The fundamental questions related to the multi-agent formation are 1) how to perform network localization to provide information that meets the requirement of formation control, and 2) how to determine the formation control that exploits the estimated positions of agents to adjust the network geometry. The performance of the multi-agent formation is determined interactively by both procedures, and thus can benefit from integrated design of the strategies, which can lead to more rational localization executions and control algorithms.

There are some studies on each individual topic. On the one hand, most existing methods of formation control mainly

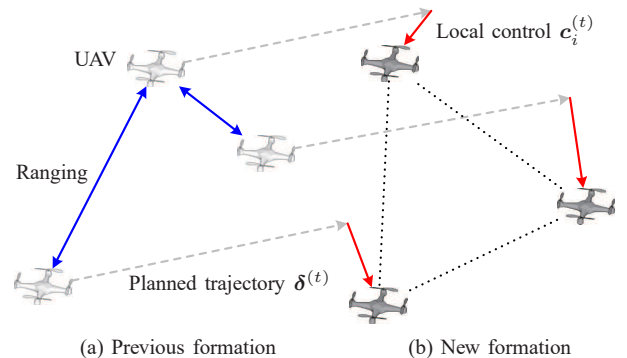


Fig. 1. A squad of three UAVs with the target formation an equilateral triangle. The multi-agent system moves along a planned trajectory $\delta^{(t)}$ at each time slot, and manages to maintain the geometry by two steps: 1) agents update their position estimations by ranging measurements, and 2) each agent adjusts its position locally based on estimations of the entire formation.

focus on the stability, rather than the accuracy of the network formation [4], [5]. The performance of a control algorithm is either evaluated by the rate of convergence to the target formation, or the deviation of the true trajectory from the planned one. However, these metrics do not directly reflect how close the real formation is to the target formation. On the other hand, current studies usually design link selection strategies to enhance the absolute network localization under limited spectrum resource [6], [7], while the performance of network formation is determined by relative positions. It also differs from the relative positioning error [8], [9], since we make the evaluation on the real network, which is affected by not only network localization, but also formation control. To sum up, a new metric is needed to characterize the accuracy of multi-agent formation, and we should consider the integration of localization and control in the design of strategies.

In this paper, we investigate high-accuracy multi-agent formation under limited spectrum resource. The main contributions are summarized as follows:

- We propose a metric called formation error to characterize the minimum squared error between a real formation and a target one over arbitrary translation and rotation.
- We establish a general framework for the multi-agent

formation, and develop an integrated localization and control scheme to enhance the performance.

- We design the minimum mean formation error (MMFE) control algorithm along with a specific link selection strategy in the case study.

Notations: The n -dimensional real number space is denoted by \mathbb{R}^n . Vector (matrix) is denoted by bold lowercase (capital) letter \mathbf{x} (\mathbf{A}). Specially, \mathbf{I}_N is the identity matrix of order N , and $\mathbf{1}_N$ is the $N \times 1$ vector with all elements being 1. $[\cdot]^T$, $[\cdot]^{-1}$ and $\text{tr}\{\cdot\}$ denote the transpose, inverse and trace of its argument, respectively. $\mathcal{N}(\boldsymbol{\mu}, \boldsymbol{\Sigma})$ denotes the normal distribution with mean value $\boldsymbol{\mu}$ and covariance matrix $\boldsymbol{\Sigma}$.

II. SYSTEM MODEL

Consider a network with N agents on the two dimensional plane for T time slots. Denote the position of the i th agent at time slot t by $\mathbf{x}_i^{(t)} \in \mathbb{R}^2$, and its estimation by $\hat{\mathbf{x}}_i^{(t)}$. Define the *formation* of the network as a column vector $\mathbf{x}^{(t)} \in \mathbb{R}^{2N}$ including the positions of all agents in it, namely

$$\mathbf{x}^{(t)} = [\mathbf{x}_1^{(t)T} \quad \mathbf{x}_2^{(t)T} \quad \cdots \quad \mathbf{x}_N^{(t)T}]^T. \quad (1)$$

There may also exist some anchors with known positions, which can aid the agents in localization.

The objective of the multi-agent formation is to conform the real network with the target geometry. A *target formation* $\boldsymbol{\xi} \in \mathbb{R}^{2N}$ is defined by including the target positions of all agents $\{\boldsymbol{\xi}_i \in \mathbb{R}^2\}$ in the column vector,¹ and it is assumed to be constant during the observed period.

A. Physical Control Model

The movement of each agent can be divided into two parts. First, the entire formation moves along a planned trajectory $\boldsymbol{\delta}^{(t)}$ at time slot t , which is a global displacement and known to all agents, to accomplish certain tasks. Second, each agent performs a local control $\mathbf{c}_i^{(t)}$ on its own position to conform the real network with the target formation.² Thus the location of agent i at time slot t is given by

$$\mathbf{x}_i^{(t)} = \mathbf{x}_i^{(t-1)} + [\boldsymbol{\delta}^{(t)} + \mathbf{c}_i^{(t)} + \mathbf{w}_i^{(t)}] \quad (2)$$

where $\mathbf{w}_i^{(t)} \sim \mathcal{N}(\mathbf{0}, \sigma_c^2 \mathbf{I}_2)$ is independently and identically distributed (i.i.d.) for each agent. We further define that

$$\mathbf{c}^{(t)} = [\mathbf{c}_1^{(t)T} \quad \mathbf{c}_2^{(t)T} \quad \cdots \quad \mathbf{c}_N^{(t)T}]^T \quad (3)$$

$$\mathbf{w}^{(t)} = [\mathbf{w}_1^{(t)T} \quad \mathbf{w}_2^{(t)T} \quad \cdots \quad \mathbf{w}_N^{(t)T}]^T. \quad (4)$$

B. State Inference Model

For location inference, the agents perform distance measurements with neighboring nodes by technologies such as round-trip time (RTT). The distance measurement between agent i and j at time slot t is modeled as

$$d_{ij}^{(t)} = \|\mathbf{x}_i^{(t)} - \mathbf{x}_j^{(t)}\| + v_{ij}^{(t)} \quad (5)$$

¹The target formation is not unique because of translation and rotation, and thus it is a set rather than a single vector (see Section III). Such expression just denotes a realization of the target formation.

²In practical systems, control on the acceleration can be derived by designing the corresponding double integrator controller [10].

where $v_{ij}^{(t)} \sim \mathcal{N}(0, \sigma_r^2)$ denotes the ranging noise, assumed to be i.i.d. for different ranging links. Suppose that each time slot can be divided into L resource units (RU), and only one ranging link is set up in the entire network for each RU.

The agents can update the position estimations based on the state evolution model (2) and distance measurements (5) by various approaches. Particularly, this paper employs the method of particle filter [11]. The number of particles used to describe the position distribution is proportional to $|\hat{\boldsymbol{\Sigma}}_i^{(t)}|^{1/2}$, where $\hat{\boldsymbol{\Sigma}}_i^{(t)}$ is the estimated covariance matrix of $\hat{\mathbf{x}}_i^{(t)}$.

III. FRAMEWORK FOR MULTI-AGENT FORMATION

In this section, we propose a new metric called *formation error* to characterize the difference between a real formation and a target one over arbitrary translation and rotation, and establish a general framework for the multi-agent formation.

A. Performance Metric

In the problem of the multi-agent formation, we adjust the real network towards the target geometry, as is presented in the target formation $\boldsymbol{\xi}$. The goal is realized as long as the formation after control can be achieved by applying certain translation and rotation operators to the target formation $\boldsymbol{\xi}$. Thus the objective of the multi-agent formation is actually a set, rather than a vector, which is different from many other problems of parameter estimation where the squared error is usually employed as the performance metric.

Definition 1: The set including all target formations, which can be achieved by applying translation and rotation to $\boldsymbol{\xi}$, is called the *feasible set* and is denoted by $\mathcal{S} = \mathcal{S}(\boldsymbol{\xi})$.

According to Definition 1, each element in the feasible set can be realized as follows: 1) set the initial formation as the target formation $\boldsymbol{\xi}$, 2) rotate the entire formation by some angle $\vartheta \in [0, 2\pi)$, and 3) translate each agent by some vector $\mathbf{t} \in \mathbb{R}^2$. Thus the feasible set can be presented as

$$\mathcal{S}(\boldsymbol{\xi}) = \{[\mathbf{I}_N \otimes \mathbf{R}(\vartheta)]\boldsymbol{\xi} + \mathbf{1}_N \otimes \mathbf{t}\} \quad (6)$$

where $\mathbf{R}(\vartheta)$ denotes the Givens matrix with angle ϑ

$$\mathbf{R}(\vartheta) = \begin{bmatrix} \cos \vartheta & -\sin \vartheta \\ \sin \vartheta & \cos \vartheta \end{bmatrix} \quad (7)$$

and \otimes is the Kronecker product. Note that the feasible set generated from any target formation is the same, and thus without loss of generality, we can assume that the target formation is centered at the origin, namely $\sum_{i=1}^N \boldsymbol{\xi}_i = \mathbf{0}$.

Definition 2: The *formation error* between formations \mathbf{x} and $\boldsymbol{\xi}$ is defined as the squared distance between vector \mathbf{x} and the feasible set $\mathcal{S} = \mathcal{S}(\boldsymbol{\xi})$, which is

$$\mathcal{F}(\mathbf{x}, \boldsymbol{\xi}) = \min_{\mathbf{s} \in \mathcal{S}} \|\mathbf{x} - \mathbf{s}\|^2. \quad (8)$$

Formation error is in fact the least squared error between the real formation and all target formations. Define the *cost of control* as the sum of squared distances that each agent moves during the procedure of formation control, then the formation error indicates the least cost of control that is needed to conform the real formation with a target one for the entire

system. For a more intuitive understanding of the formation error, the root averaged formation error can be defined as

$$\text{RAFE}(\mathbf{x}, \boldsymbol{\xi}) = \sqrt{\mathcal{F}(\mathbf{x}, \boldsymbol{\xi})/N} \quad (9)$$

which roughly describes the least averaged distance each agent needs to move to conform with the target formation.

Proposition 1: The formation error between formations \mathbf{x} and $\boldsymbol{\xi}$ is given by

$$\mathcal{F}(\mathbf{x}, \boldsymbol{\xi}) = \|\mathbf{D}\mathbf{x}\|^2 + \|\boldsymbol{\xi}\|^2 - 2\|\boldsymbol{\xi}\| [\mathbf{x}^\top (\mathbf{D}\mathbf{P}\mathbf{D})\mathbf{x}]^{1/2} \quad (10)$$

where

$$\mathbf{D} = \mathbf{I}_{2N} - \frac{1}{N}(\mathbf{1}_N \mathbf{1}_N^\top) \otimes \mathbf{I}_2 \quad (11)$$

and the projection matrix

$$\mathbf{P} = \frac{1}{\|\boldsymbol{\xi}\|^2}(\boldsymbol{\xi}\boldsymbol{\xi}^\top + \boldsymbol{\eta}\boldsymbol{\eta}^\top) \quad (12)$$

with another target formation $\boldsymbol{\eta} = [\mathbf{I}_N \otimes \mathbf{R}(\pi/2)]\boldsymbol{\xi}$.

Proof: Since the feasible set can be expressed as (6), the formation error follows that

$$\mathcal{F}(\mathbf{x}, \boldsymbol{\xi}) = \min_{\mathbf{t}, \vartheta} \left\{ \sum_{i=1}^N \|\mathbf{x}_i - \mathbf{R}(\vartheta)\boldsymbol{\xi}_i - \mathbf{t}\|^2 \right\}. \quad (13)$$

Set both derivatives with respect to \mathbf{t} and ϑ as zero, and the optimal translation and rotation are given by

$$\{\mathbf{t}^*, \vartheta^*\} = \left\{ \frac{1}{N} \sum_{i=1}^N \mathbf{x}_i, \arctan \left[\frac{\boldsymbol{\eta}^\top (\mathbf{x} - \mathbf{t}^*)}{\boldsymbol{\xi}^\top (\mathbf{x} - \mathbf{t}^*)} \right] \right\}. \quad (14)$$

Then the formation error (10) can be derived by substituting (14) into (13), using $\mathbf{R}(\vartheta) = \mathbf{I} \cos \vartheta + \mathbf{R}(\pi/2) \sin \vartheta$. \square

Matrix \mathbf{D} denotes the operation that translates the entire formation until its mass center is located at the origin, which can eliminate the influence of translation. For the convenience of notation, we define $\mathbf{y} = \mathbf{D}\mathbf{x}$ in the rest of this paper.

B. Geometrical Interpretation

Note that formation $\boldsymbol{\eta}$ can be achieved by rotating the formation $\boldsymbol{\xi}$ for $\vartheta = \pi/2$, which implies $\boldsymbol{\xi}^\top \boldsymbol{\eta} = 0$. Matrix \mathbf{P} denotes the operation that projects a formation onto the two-dimensional subspace $\mathcal{P} = \text{span}\{\boldsymbol{\xi}, \boldsymbol{\eta}\}$, where vectors $\{\boldsymbol{\xi}, \boldsymbol{\eta}\}$ can be regarded as a set of orthogonal basis for \mathcal{P} .

Proposition 2: The subset of $\mathcal{S}(\boldsymbol{\xi})$, which includes all target formations with mass centers at the origin, is a circle of radius $\|\boldsymbol{\xi}\|$ centered at the origin in the hyperplane \mathcal{P} .

Proof: Since the mass center is constrained at the origin, such a target formation $\boldsymbol{\zeta}$ can be expressed as

$$\boldsymbol{\zeta} = [\mathbf{I}_N \otimes \mathbf{R}(\vartheta)]\boldsymbol{\xi} = [\boldsymbol{\xi} \quad \boldsymbol{\eta}] \begin{bmatrix} \cos \vartheta & \sin \vartheta \end{bmatrix}^\top. \quad (15)$$

Thus $\boldsymbol{\zeta} \in \mathcal{P}$ and $\|\boldsymbol{\zeta}\| = \|\boldsymbol{\xi}\|$. Vice versa. \square

An equivalent form for formation error (10) is given in the following proposition, which is derived from the perspective of subspaces and induces a geometric interpretation.

Proposition 3: The formation error can be decomposed as

$$\mathcal{F}(\mathbf{x}, \boldsymbol{\xi}) = \|\mathbf{y}_\perp\|^2 + (\|\mathbf{y}_\parallel\| - \|\boldsymbol{\xi}\|)^2 \quad (16)$$

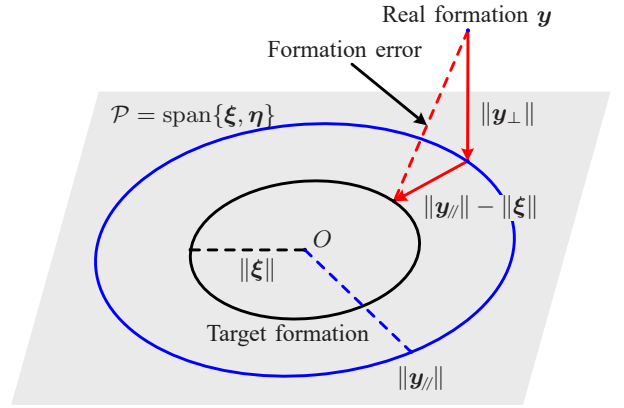


Fig. 2. The decomposition of formation error. The parallel error is the squared distance between the projection of \mathbf{y} on \mathcal{P} and the circle of target formations; the vertical error is the squared distance from \mathbf{y} to \mathcal{P} .

where $\mathbf{y}_\parallel = \mathbf{P}\mathbf{y}$ and $\mathbf{y}_\perp = (\mathbf{I} - \mathbf{P})\mathbf{y}$ are respectively the components of formation \mathbf{y} in subspace \mathcal{P} and its orthogonal complementary \mathcal{P}^\perp .

Proof: By the orthogonal projection theorem, formation \mathbf{y} can be decomposed as \mathbf{y}_\parallel within the range and \mathbf{y}_\perp within the kernel of projection \mathbf{P} . It then follows that

$$\|\mathbf{y}\|^2 = \|\mathbf{y}_\parallel\|^2 + \|\mathbf{y}_\perp\|^2 \quad (17)$$

and since \mathbf{P} is both symmetric and idempotent,

$$\mathbf{y}^\top \mathbf{P}\mathbf{y} = [\mathbf{P}\mathbf{y}]^\top [\mathbf{P}\mathbf{y}] = \|\mathbf{y}_\parallel\|^2. \quad (18)$$

Substituting the above terms into (10) leads to (16). \square

As Fig. 2 shows, the formation error (16) can be decomposed into two parts, each of which is separately determined by the components of the formation \mathbf{y} in the corresponding subspaces, namely \mathbf{y}_\perp and \mathbf{y}_\parallel , and we call them the vertical error and the parallel error, respectively. Specially, the parallel error is the squared distance from \mathbf{y}_\parallel to the circle of target formations, and is free of the direction of \mathbf{y}_\parallel . Thus the effect of rotation is eliminated in the metric of formation error.

C. General Framework

As a typical application of cyber-physical systems (CPS), multi-agent formation can generally be realized by three steps – *environment sensing*, *state estimation* and *formation control*, and strategies \mathcal{A} , \mathcal{E} and \mathcal{C} are respectively applied in each step. Specially, the network state $\mathbf{x}^{(t)}$ refers to the positions of all agents in the multi-agent system.

First, for better estimation of the current network state, the resource, such as power or spectrum, is allocated based on the target formation and previous estimation $\hat{\mathbf{x}}^{(t-1)}$ by strategy \mathcal{A} , and the measurements $\mathbf{m}^{(t)}$ are obtained. Next, information fusion of the state evolution and observations is realized by method \mathcal{E} to update the estimated network state. Finally, control vector $\mathbf{c}^{(t)}$ is generated from policy \mathcal{C} based on the estimation and the target formation so that the real formation of the multi-agent system is rationally adjusted.

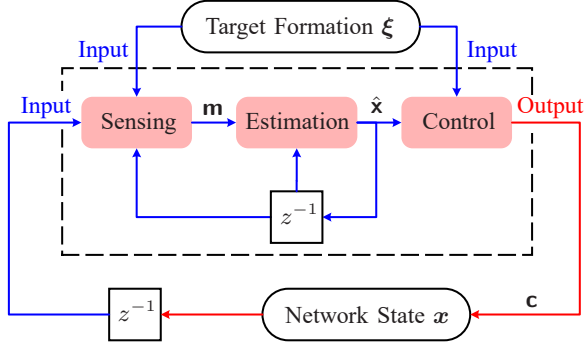


Fig. 3. The general framework for high-accuracy multi-agent formation, where z^{-1} denotes the unit of time delay. The existence of the target formation affect both the sensing phase and the control phase.

Due to uncertainty of measurements and control, the output formation is a random vector. The sequence of real formations $\{\mathbf{x}^{(t)}\}$ is a stochastic process, and the state evolves by

$$\mathbf{x}^{(t)} = \mathbf{x}^{(t-1)} + \mathbf{c}^{(t)}(\hat{\mathbf{x}}^{(t)}(\mathbf{m}^{(t)})) + \mathbf{w}^{(t)}. \quad (19)$$

To evaluate the average performance of the network formation under certain combination of strategies $\{\mathcal{A}, \mathcal{E}, \mathcal{C}\}$, the mean formation error (MFE) is then defined as

$$F^{(t)}(\{\mathcal{A}, \mathcal{E}, \mathcal{C}\}) = \mathbb{E}\{\mathcal{F}(\mathbf{x}^{(t)}, \xi)\} \quad (20)$$

for time slot t , and the time-averaged MFE follows that

$$F(\{\mathcal{A}, \mathcal{E}, \mathcal{C}\}) = \frac{1}{T} \sum_{t=1}^T F^{(t)}(\{\mathcal{A}, \mathcal{E}, \mathcal{C}\}) \quad (21)$$

which can characterize the stability of multi-agent formation as the length of observed period $T \rightarrow \infty$.

IV. INTEGRATED LOCALIZATION AND CONTROL

In order to improve the accuracy of multi-agent formation, we advocate joint optimization over the separate procedures presented in Fig. 3, and an integrated localization and control scheme is proposed as follows.

A. Motivation for Integration

The performance of the multi-agent formation can benefit from integrated design of localization and control. We can manipulate the execution of network localization by designing the strategy of link selection. The optimal integrated localization and control approach refers to

$$\{\mathcal{A}, \mathcal{C}\}^* = \arg \min_{\mathcal{A}, \mathcal{C}} F(\{\mathcal{A}, \mathcal{E}_0, \mathcal{C}\}) \quad (22)$$

where \mathcal{E}_0 is a given estimation method. Benefits of integrated strategy design are twofold. First, to design the control policy, we can refine assumptions on the inputs (estimated network state) by analyzing the link selection strategy. Second, in the design of link selection, we can consider the integration of its outputs (set of selected links) with the control policy.

B. Integrated Strategy Design

We then follow the principle of the proposed integrated scheme to design an execution of network localization (link selection), in order to aid a specific control policy.

1) *Control Policy*: We first design the minimum MFE control when the real formation \mathbf{x} is given. The goal is to achieve least MFE in the presence of control error, and we aim for lowest cost of control once the goal is attained. With control vector \mathbf{c} and error \mathbf{w} , the MFE can be derived as³

$$F = \mathbb{E}\{\mathcal{F}(\mathbf{x} + \mathbf{c} + \mathbf{w}, \xi)\} = \|\mathbf{y}_\perp + \mathbf{c}_\perp\|^2 + h(\|\mathbf{y}_\parallel + \mathbf{c}_\parallel\|^2) + (2N - 2)\sigma_c^2 \quad (23)$$

where \mathbf{c}_\perp and \mathbf{c}_\parallel are the components of the control vector in subspaces \mathcal{P}^\perp and \mathcal{P} , and we define that for $\nu \geq 0$,

$$h(\nu) = \nu - \sqrt{2\pi}\sigma_c \|\xi\| L_{1/2}\left(-\frac{\nu}{2\sigma_c^2}\right) + \|\xi\|^2 \quad (24)$$

with $L_{1/2}(\cdot)$ denoting the $1/2$ order Laguerre polynomial. Note that $h(\nu)$ attains its minimum at $\nu = \rho^2$ where

$$\rho = \left[\max\left\{-2\sigma_c^2 g\left(-\frac{2\sigma_c}{\sqrt{2\pi}\|\xi\|}\right), 0\right\} \right]^{1/2} \quad (25)$$

with $g(\cdot)$ the inverse function of first derivative of $L_{1/2}(\cdot)$.

Since \mathbf{c}_\perp and \mathbf{c}_\parallel are not interacted in (23), we can design them separately in order to minimize the MFE. On the one hand, the MFE is affected by component \mathbf{c}_\perp via $\|\mathbf{y}_\perp + \mathbf{c}_\perp\|^2$, which directly leads to $\mathbf{c}_\perp = -\mathbf{y}_\perp$. On the other hand, the component \mathbf{c}_\parallel is optimal for reducing the MFE as long as $\|\mathbf{y}_\parallel + \mathbf{c}_\parallel\| = \rho$. To sum up, the *optimal control set* whose element can achieve the least MFE is given by

$$\mathcal{C} = \left\{ \frac{\rho}{\|\xi\|} (\xi \cos \alpha + \eta \sin \alpha) - \mathbf{y} \mid \alpha \in [0, 2\pi) \right\}. \quad (26)$$

Among the control vectors in (26), the minimum cost of control is achieved when $\alpha^* = \arctan(\eta^T \mathbf{y}_\parallel / \xi^T \mathbf{y}_\parallel)$. Hence, given the real formation \mathbf{x} , the MMFE control is

$$C^*(\mathbf{x}) = \rho \frac{PD\mathbf{x}}{\|PD\mathbf{x}\|} - D\mathbf{x} \quad (27)$$

which utilizes $\hat{\mathbf{x}}$ instead of \mathbf{x} in practical implements.

2) *Sensing Strategy*: We then develop a specific strategy of link selection to aid the performance of MMFE control, when the real formation is unknown and we need to estimate the agents' positions. This strategy is designed for scenarios where 1) control uncertainty $\sigma_c \ll \|\xi\|$, and 2) the estimated formation $\hat{\mathbf{x}}$ is of high accuracy. The MFE can be derived as

$$F = \mathbb{E}\{\mathcal{F}(\mathbf{x} + C^*(\hat{\mathbf{x}}) + \mathbf{w}, \xi)\} = \mathbb{E}\{\|\mathbf{y} - \hat{\mathbf{y}}\|^2\} + (\rho - \|\xi\|)^2 + (2N - 2)\sigma_c^2 + \tilde{F} \quad (28)$$

where

$$\tilde{F} = -2\|\xi\| \mathbb{E}\{\|\mathbf{y}_\parallel + \rho \hat{\mathbf{y}}_\parallel / \|\hat{\mathbf{y}}_\parallel\| - \hat{\mathbf{y}}_\parallel + D\mathbf{w}_\parallel\|\} + 2\|\xi\| \rho + 2\rho \mathbb{E}\{(\mathbf{y}_\parallel - \hat{\mathbf{y}}_\parallel)^T \hat{\mathbf{y}}_\parallel / \|\hat{\mathbf{y}}_\parallel\|\}. \quad (29)$$

³Note that the error resulted from control uncertainty is reduced by $2\sigma_c^2$, since in MFE we apply the operation D to eliminate the effect of translation, which is described by two dimensions for a plane formation.

Under the assumptions above, the arguments of the expectation operator in the first and last terms of (29) can be approximated by the second-order Taylor polynomials of the corresponding functions at $\hat{\mathbf{y}}_{//} = \mathbf{y}_{//}$, which leads to an approximated form of the MFE defined in (28) as follows

$$F_A = \mathbb{E}\{(\mathbf{y} - \hat{\mathbf{y}})^T \mathbf{B}(\mathbf{y} - \hat{\mathbf{y}})\} + F_c. \quad (30)$$

The term F_c denotes the part of error resulted from control uncertainty, which is defined as

$$F_c = (\rho - \|\boldsymbol{\xi}\|)^2 + \left(2N - 2 - \frac{\|\boldsymbol{\xi}\|}{\rho}\right) \sigma_c^2. \quad (31)$$

The weight matrix in the first term of (30) is given by

$$\mathbf{B} = \mathbf{I}_{2N} - \left[\frac{\|\boldsymbol{\xi}\|}{\rho} - \frac{2(\|\boldsymbol{\xi}\| - \rho)}{\|\mathbf{y}_{//}\|} \right] \frac{\mathbf{y}_\tau \mathbf{y}_\tau^T}{\|\mathbf{y}_\tau\|^2} \quad (32)$$

where $\mathbf{y}_\tau = [(\boldsymbol{\xi}\boldsymbol{\xi}^T - \boldsymbol{\eta}\boldsymbol{\xi}^T)/\|\boldsymbol{\xi}\|^2]\mathbf{y}$ lies in the subspace \mathcal{P} and is perpendicular to $\mathbf{y}_{//}$, and denotes the dimension of rotation operator, which is free of concern in multi-agent formation.

Proposition 4: In the presence of ranging and control uncertainty, the approximated MFE is lower bounded by

$$F_A \geq \text{tr}\{\mathbf{B}\mathbf{D}\mathbf{J}^{-1}(\mathbf{x})\} + F_c \quad (33)$$

where $\mathbf{J}(\mathbf{x})$ denotes the Fisher information matrix (FIM) for formation \mathbf{x} based on the state evolution and observations.

Proof: According to the information inequality, the mean squared positioning error (SPE) is lower bounded by [12]

$$\mathbb{E}\{(\mathbf{x} - \hat{\mathbf{x}})(\mathbf{x} - \hat{\mathbf{x}})^T\} \succeq \mathbf{J}^{-1}(\mathbf{x}). \quad (34)$$

Transformation of parameters leads to (33). \square

We develop the link selection strategy in order to minimize the theoretical bound. Denote the FIM at the beginning of the RU by $\mathbf{J}_0(\mathbf{x})$, and the FIM when the ranging link (i, j) is set up by $\mathbf{J}_{i,j}(\mathbf{x})$. The *weight* of link (i, j) is defined as the reduction of (33) due to its existence, namely

$$v_{i,j} = \text{tr}\{\mathbf{B}\mathbf{D}[\mathbf{J}_0^{-1}(\mathbf{x}) - \mathbf{J}_{i,j}^{-1}(\mathbf{x})]\}. \quad (35)$$

The link with largest weight is optimal in resource utility for error reduction, and will be set up for the RU.⁴

Remark 1: The lower bound (33) contains two parts. The first part exhibits the effect of positioning uncertainty, where the SPEs of the agents are weighted by $\mathbf{B}\mathbf{D}$. The second part (31) indicates the effect of control uncertainty, which can be interpreted as the bias and variance decomposition, where variance on all directions is concerned except those implying translation and rotation (totally three dimensions).

Remark 2: The lower bound (33) is affected by uncertainties of control σ_c^2 and ranging σ_r^2 in an intricate way, since the positioning error is jointly determined by the uncertainty of state evolution and observation. In a special case where $\sigma_c \gg \sigma_r$, the observations can provide more accurate information than the state evolution, and the SPE will be almost proportional to σ_r^2 and free of σ_c^2 , leading to MFE exhibiting a linear growth with both parameters.

⁴In practice, approximated FIM and weight matrix \mathbf{B} calculated from the estimated formation are used in (35) for the implement of this procedure.

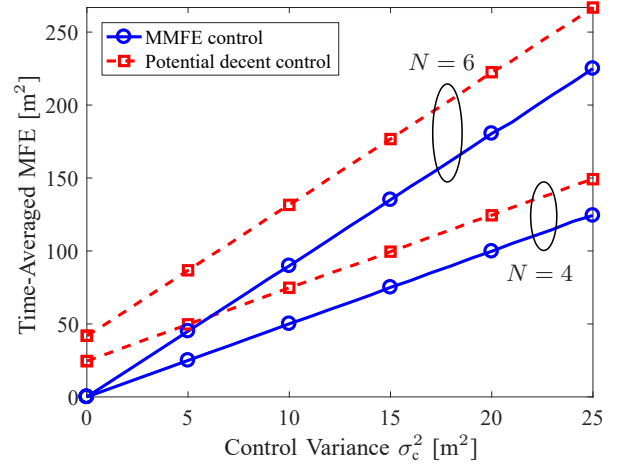


Fig. 4. Compared with the potential decent control, MMFE control attains lower MFE, and the gap grows with the number of UAVs.

V. NUMERICAL RESULTS

Consider a squad of N UAVs on a plane for $T = 10^3$ time slots. The planned trajectory is set as $\delta^{(t)} = [0 \ 5]^T$ m for all time slots. The set of anchors' positions is a homogeneous Poisson point process (PPP) with $\lambda = 5 \times 10^{-5}$ m⁻². The target formation is a uniform line with the distance between adjacent agents being 20 m. The communication range is $R = 100$ m, and the number of RUs is set as $L = N$.

A. Control Policy

We compare the MMFE control with the potential decent control, where the target position of agent i is given by [5]

$$\mathbf{x}_i^* = \arg \min_{\mathbf{x}} \sum_{j \neq i} (\|\mathbf{x} - \mathbf{x}_j\|^2 - \|\boldsymbol{\xi}_i - \boldsymbol{\xi}_j\|^2)^2. \quad (36)$$

The real formation $\mathbf{x} \sim \mathcal{N}((\mathbf{R}(\beta) \otimes \mathbf{I}_N)\boldsymbol{\xi}, \mathbf{I}_{2N})$ m is known, where $\beta \sim \mathcal{U}[0, 2\pi)$ is a random orientation. We consider two scenarios, where the numbers of UAVs are $N = 4$ and $N = 6$, and the control uncertainty is $\sigma_c^2 = 1$ m² for both cases.

First, we compare the time-averaged MFE of both methods in Fig. 4. The MMFE control achieves lower MFE than the potential decent control, and the performance gap increases as the size of formation grows. Second, we compare the mean cost of control, namely $\mathbb{E}\{\|\mathbf{c}\|^2\}$, of the methods. The MMFE control requires lower cost, namely 21 m² and 29 m², than the potential decent control (100 m² and 124 m²). Finally, the time complexity of MMFE control is two orders of magnitude lower than the potential decent control for both scenarios, since the MMFE control has a closed-form expression that can be implemented without iterations, and thus it exhibits higher capability in real-time tasks.

B. Link Selection

We then compare the performance of the proposed link selection strategy and random selection, in scenarios where the number of UAVs ranges from 4 to 20, and $\sigma_c^2 = \sigma_r^2 = 1$ m². The MMFE control is adopted for all cases.

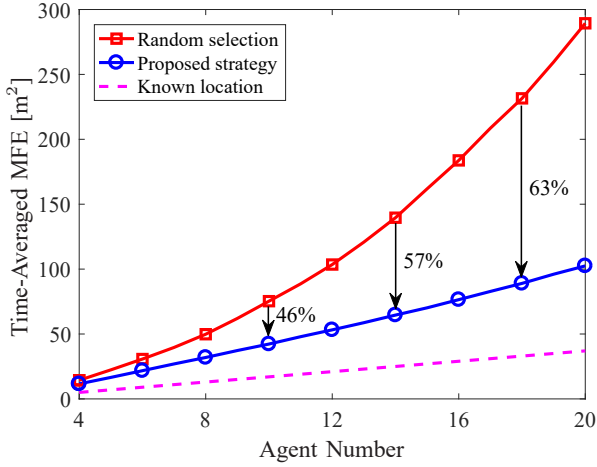


Fig. 5. The time-averaged MFE under the proposed strategy increases linearly with the size of formation, and outperforms that of random selection, which results in an increasing averaged MFE per agent as agent number grows.

As shown in Fig. 5, under the proposed strategy, the time-averaged MFE is proportional to the number of agents. However, under random selection, the share of the time-averaged MFE in each agent increases with the size of formation, from which it is reasonable to infer that random selection is not capable of maintaining the geometry in applications requiring large multi-agent systems. We also present the performance curve when the precise formation is provided, which serves as the baseline for all link selection strategies.

C. System Parameters

We finally investigate the effects of system parameters on the time-averaged MFE in a formation of $N = 4$ UAVs, with various control uncertainty σ_c^2 and ranging uncertainty σ_r^2 in different scenarios. The MMFE control policy and the proposed link selection strategy are employed.

The results are shown in Fig. 6. First, the MFE increases sub-linearly with the ranging uncertainty σ_r^2 due to the state evolution model, which constrains the growth of the SPE with σ_r^2 , especially under precise control. Second, the MFE increases almost linearly with the control uncertainty σ_c^2 , which includes the growth of the error resulted from control uncertainty and the increment of the positioning error. The results provide us some intuitive understanding about the effects of the system parameters, and can serve as a guideline for practical system design.

VI. CONCLUSION

In this paper, we established a general framework for high-accuracy multi-agent formation. We first proposed a new metric called formation error to characterize the minimum squared distance between a real formations and a target one over arbitrary translation and rotation. Then we developed an integrated localization and control scheme to minimize the formation error, and designed the MMFE control algorithm along with a specific link selection strategy in the case study.

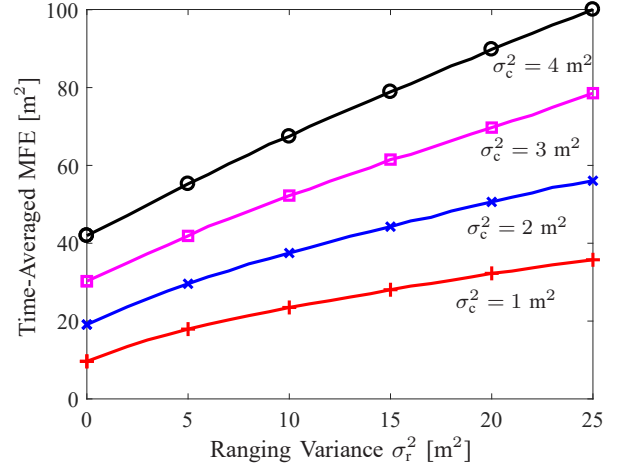


Fig. 6. The time-averaged MFE increases sub-linearly with the ranging uncertainty σ_r^2 , and almost linearly with the control uncertainty σ_c^2 . When $\sigma_c^2 \gg \sigma_r^2$, it grows almost linearly with both parameters.

Numerical results were presented to validate the performance gain of the proposed methods, and demonstrated the effects of the control and the measurement uncertainty, which can serve as a guideline for the design of practical systems.

VII. ACKNOWLEDGMENT

This research was supported in part, by the National Natural Science Foundation of China under Grant 61501279 and 91638204.

REFERENCES

- [1] X. Dong, B. Yu, Z. Shi, and Y. Zhong, "Time-varying formation control for unmanned aerial vehicles: Theories and applications," *IEEE Trans. Control Syst. Technol.*, vol. 23, no. 1, pp. 174–188, Jan. 2015.
- [2] D. J. Pack, P. DeLima, G. J. Toussaint, and G. York, "Cooperative control of UAVs for localization of intermittently emitting mobile targets," *IEEE Trans. Syst., Man, Cybern.*, vol. 39, no. 4, pp. 959–970, Aug. 2009.
- [3] M. Z. Win, A. Conti, S. Mazuelas, Y. Shen, W. M. Gifford, D. Dardari, and M. Chiani, "Network localization and navigation via cooperation," *IEEE Commun. Mag.*, vol. 49, no. 5, pp. 56–62, May 2011.
- [4] K. K. Oh, M. C. Park, and H. S. Ahn, "A survey of multi-agent formation control," *Automatica.*, vol. 53, no. s, pp. 424–440, Mar. 2015.
- [5] M. Cao, C. Yu, and B. D. Anderson, "Formation control using range-only measurements," *Automatica.*, vol. 47, no. 4, pp. 776–781, Apr. 2011.
- [6] T. Wang, Y. Shen, A. Conti, and M. Z. Win, "Network navigation with scheduling: Error evolution," *IEEE Trans. Inf. Theory*, vol. 63, no. 11, pp. 7509–7534, Nov. 2017.
- [7] T. Lv, H. Gao, X. Li, S. Yang, and L. Hanzo, "Space-time hierarchical-graph based cooperative localization in wireless sensor networks," *IEEE Trans. Signal Process.*, vol. 64, no. 2, pp. 322–334, Jan. 2016.
- [8] J. N. Ash and R. L. Moses, "On the relative and absolute positioning errors in self-localization systems," *IEEE Trans. Signal Process.*, vol. 56, no. 11, pp. 5668 – 5679, Jun. 2008.
- [9] N. Patwari, A. O. Hero, M. Perkins, N. S. Correal, and R. J. O’Dea, "Relative location estimation in wireless sensor networks," *IEEE Trans. Signal Process.*, vol. 51, no. 8, pp. 2137 – 2148, Aug. 2003.
- [10] V. G. Rao and D. S. Bernstein, "Naive control of the double integrator," *IEEE Control Syst. Mag.*, vol. 21, no. 5, pp. 86 – 97, Oct. 2001.
- [11] M. S. Arulampalam, S. Maskell, N. Gordon, and T. Clapp, "A tutorial on particle filters for online nonlinear/non-Gaussian Bayesian tracking," *IEEE Trans. Signal Process.*, vol. 50, no. 2, pp. 174–188, Feb. 2002.
- [12] Y. Shen, H. Wymeersch, and M. Z. Win, "Fundamental limits of wideband localization – Part II: Cooperative networks," *IEEE Trans. Inf. Theory*, vol. 56, no. 10, pp. 4981–5000, Oct. 2010.